Host−Dopant System To Generate Bright Electroluminescence from Small Organic Molecule Functionalized Light-Emitting Electrochemical Cells

Madayanad Suresh Subeesh,[†] Kanagaraj Shanmugasundaram,[†] Chozhidakath Damodharan Sunesh,[†] Ramesh Kumar Chitumalla,[‡] Joonkyung Jang,[‡] and Youngson Choe*,[†]

[†]Department of Polymer Science and Chemical Engineering, and [‡]Department of Nanoenergy Engineering, Pusan National University, Busan 609-735, South Korea

S *Supporting Information*

ABSTRACT: Albeit their easy accessibility and low cost, small organic molecules are not known for their high electroluminescence in light-emitting electrochemical cells (LECs). To construct a bright low-cost LEC device, the functions of charge transport and charge recombination should be separated in the active layer of LEC devices. Herein, we demonstrate that the widely used host−dopant strategy in organic light-emitting diodes (OLEDs) can significantly improve the electroluminescence from small organic molecule fueled LEC devices, provided the host molecules are carefully selected. Furthermore, performance of host−dopant small-molecule LEC devices hugely relies on the properties of host materials rather than the emitting luminophores. Conversely to the high performance of intramolecular charge-transfer (ICT) molecular systems in OLEDs, doped ICT fluorophores having a low-lying charge-transfer state can behave like exciton loss channels in the high ionic environment of LEC-active layers. Similar to the behavior of previously reported ICT molecules in polar solvents, our synthesized D−π-A−π-D phenanthroimidazole derivative exhibited fluorescence quenching and a huge blue shift of emission in the doped thin film of the ionic host. However, even with a less efficient emitter, high electroluminescence was achieved from a host−dopant LEC system. Our best device exhibited a maximum brightness of 5016 cd/m^2 at a current efficiency of 0.73 cd/A. This device outplays our previously reported nondoped LEC (ihpypn-LEC) with a 7-fold increase in the maximum brightness and over a 3-fold increase in the current efficiency at peak brightness. To the best of our knowledge, these peak brightness values recorded here (device 2) are the best among those reported by small organic molecule LEC devices so far. This report reveals the potential of small organic molecules, especially phenanthroimidazole derivatives, in casting bright and efficient low-cost host−dopant LECs with minimum effort and appreciable sustainability.
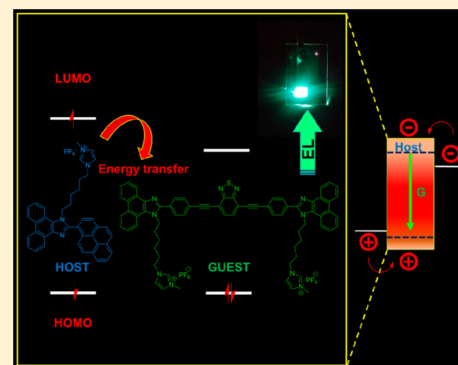
INTRODUCTION

The technological revolutions in the lighting area for the past few years have been fueled mainly by significant findings in organic semiconductor materials, especially those materials applicable in organic light-emitting diodes.[1−3] The urge for low-cost solid-state lighting has strengthened at present more than ever before. As a result, one could even anticipate the comeback of the world's cheapest lighting source ever, the incandescent lamp, in a totally different outlook. Within a decade or so, a huge part of the point lighting sources used at present will be replaced by flat panel eye-friendly lighting devices, and the impact of these changes will be a huge relief on the increasing global energy demand. For the establishment of low-cost lighting techniques, attention has to focus on the development of cheap and sustainable materials utilizing simple lighting devices. Ever since the discovery of light-emitting electrochemical cells (LECs), a huge amount of devoted research has been focused on its development.[4] Several studies published on LECs have been construed as sufficient to validate them as

promising lighting sources.[5] Confinement of the LEC library to ionic transition metal complexes (iTMCs) and conjugated polymers is considered as a major limitation for its growth.[6] However, both of this class of emitters have achieved several promising performances under the configuration of LECs.[7−9]

Intense research on materials that can be utilized in LECs and the technological revolution in the device engineering processes have presented increased efficiency for this potential lighting application.[7,10−12] Nonetheless, LECs still lack so many features that must be achieved for a future generation lighting source. Most LEC devices reported to date are more efficient rather than being bright, not relying on the class of active materials used, achieving strong electroluminescence from LECs is still a challenging endeavor.[13] It is highly advantageous to have high luminescence from LEC devices to find its way for

Scheme 1. Synthetic Routes for ibpbn and itpbn
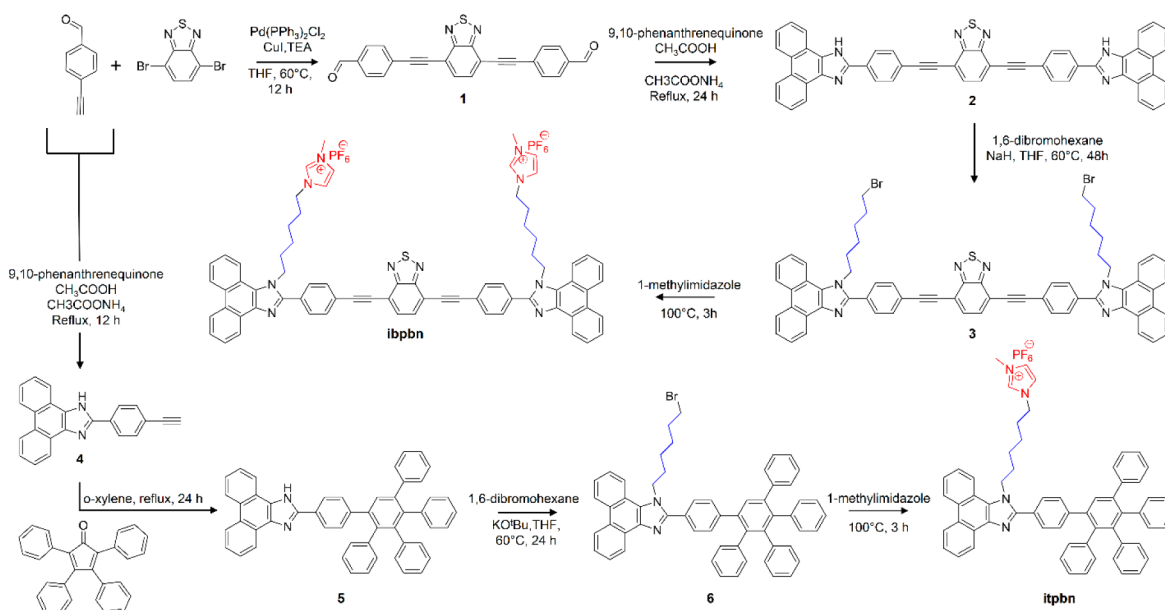
practical applications. It will be better to have a brighter, less efficient LEC device than a low-luminescent efficient device. Due to its low cost and simple manufacturing processes, with conditions, LECs can sacrifice their efficiency for brightness.[13] Even in the beginning stage, a neutral green emitting organic small-molecule-based LEC device presented a reasonable brightness of ~3000 cd/m², which clearly indicated their potential to lead the development in this area of research.[6] In this regard, very few reports have been published on conjugated polymers and iTMCs.[7,14−16] For the past few years, organic small-molecule LECs are getting much recognition at present than ever before.[13,17−19] These are progressive materials added into the LEC domain to supersede conjugated polymers and iTMCs. Furthermore, the availability of a wide range of photofunctional small organic molecule with attractive properties along with known synthetic procedures made them more open to find application in ultramodern lighting technologies.[20−22] Despite its significance, methods for utilizing organic scaffolds remain particularly underdeveloped in LECs. The loss of electrically generated dark triplet excitons in the active layer hampers the harvesting of high performance from organic small-molecule endorsed LECs.[23] To help address this technological gap, LECs can look into the recent developments in OLEDs with thermally activated delayed fluorescence (TADF) emitters.[24] However, to enhance the overall performance of the device, so many limitations still have to be resolved like high brightness, color purity, efficiency, and lifetime.[25] For satisfying all these needs, LECs can mimic the strategies that are widely used in OLEDs, viz., host−dopant system,[24] exciplex emission,[17,26] and triplet−triplet annihilation,[27] just to name a few. In sharp contrast to OLEDs, very few efforts have been made to explore these methods in LEC devices.[28] To apply the host−dopant system in LECs, identifying a suitable host material having desired properties like stable oxidized and reduced states is uttermost important to realize efficient charge injection and transport into the active layer.[29] Moreover, balanced charge transport and efficient charge transfer from host to guest have to be recognized for obtaining strong and efficient electroluminescence from guest molecules.[30]

Recent reports on small organic molecule LECs (smLECs), including ours, suggest that small organic molecular ions add much easiness in the device fabrication processes, and the intrinsic ionic nature of those materials favors single-component solution processing of the active layers.[23,31] Since device performance relies on the p−i−n junction formation during operation, optimization of mass ratios of the tricomponent blend used in the fabrication of neutral molecule based devices often turns to a complex process,[23,32] whereas small organic molecular ions can utilize their covalently bonded charged groups to satisfy the requirement for electrochemical doping and formation of the p−i−n junction during operations. Moreover, the ionic side chain incorporated molecules may show reduced intermolecular interactions in the solid state, thereby decreasing its quenching of fluorescence in the active layers.[23,32] So far, different types of molecular design and device fabrication steps have been adopted for the highest performing host−dopant LECs;[28−30] this diversity clearly indicates that an ideal multiemitter-compatible host has not yet been realized. In other words, the performance of those LEC devices is still not fully optimized. Developing a general high band gap host having enough electrochemical stability can bring about a change in the molecular design concept and performance of the next-generation LEC devices.[29]

The reports on phenanthroimidazole derivatives as host as well as nondoped blue emitters in OLEDs[20,33] along with the previous performances of these materials in LECs makes us to accord this class of compound as active material for this investigation. Like a typical host−dopant system, herein too, we selected a high-energy host and a guest having low energy. Additionally, hosts having deep-blue and sky-blue emission were selected to compare their performances. Since several factors have to be satisfied for host materials in LECs, namely, solubility and ionic nature, our selected compounds are totally different from conventional host materials used in OLEDs. All the molecules selected were designed to have ionic groups attached to the distal ends of their alkyl dendrons to make sure it can be processed from a single solvent. Donor−acceptor molecular design has been widely used in OLEDs to generate

efficient molecular scaffolds.[24] Those molecular systems are known to have a reasonably high ratio of radiative singlet excitons rather than exothermic triplets when excited electrically in photonic devices due to their high probability for reverse intersystem crossing (RISC) from the triplet state to singlet states. Importantly, the relative orientation of donor and acceptor moieties plays a nontrivial role in governing the efficiency of these molecular systems.[34] A phenanthroimidazole−benzothiadiazole-based archetypal D−π-A−π-D molecular design has been adopted for obtaining the dopant for this case. The ability of phenanthroimidazole to act like a weak electron acceptor when connected to a strong donor or weak donor when bonded with strong acceptor is utilized here for generating a D−A system.[35] Longer wavelength emission from the guest molecule is assured by including a strong electron-accepting benzothiadiazole moiety in the molecular design. Similar organic molecular systems have achieved better performance in electroluminescent devices.[21] Unfortunately, the synthesized molecule shows poor luminescence and low quantum yields, vide infra. However, even with a less efficient emitter, high electroluminescence was observed from the fabricated host−dopant LEC device. Furthermore, peak brightness values observed here are the best among reported smLECs so far.[6,13,23,28,31,36] This new strategy adopted in this report can present a new design direction toward the next generation of LEC devices, and thereby those high performance can be possible to achieve for the future generation of easily accessible, cost-effective smLECs.

■ RESULT AND DISCUSSION

Synthesis. Synthesis of ibpbn was achieved through a Sonogashira coupling of 4-ethynylbenzaldehyde and 4,7-dibromobenzo[c]-1,2,5-thiadiazole, followed by a Debus−Radziszewski synthesis to generate a D−π-A−π-D core in excellent yields (Scheme 1).[32] Alkylation of the free N$_1$ position of imidazole was tricky at low base concentrations. However, after numerous reactions, we finally found that the reaction proceeds in the presence of excess strong base in refluxing temperatures; especially, sodium hydride gives best results. The reason for this problem was found to be the presence of an electronegative ethyne bridge along with the electron-deficient acceptor moiety in the core structure, which was later confirmed by carrying out alkylation on compound **4**. The same difficulty in forming the desired product was observed in that case too. Finally the emitter, ibpbn, was obtained by introducing an imidazolium ionic group to the distal end of the side chains followed by an ion-exchange reaction with hexafluorophosphate to remove unstable and reactive bromide counterion. Like a typical phenanthroimidazole dimer, our synthesized compound also showed limited solubility in low-boiling common organic solvents.[37] However, our strategy of increasing solubility of phenanthroimidazole derivatives by incorporating ionic side chains into the core structure[23] has worked to some extent in here as well, and solubilities were observed in DMF, DMSO, 2-methoxyethanol, and 1-butanol, etc. The host **1** (ihpypn) was synthesized using our own previous report,[23] while host **2** (itpbn) was obtained through a modified previous report,[33] as shown in Scheme 1. The same method utilized in the cyclization step of our target emitter was used to obtain the key intermediate (compound **4**) in good yields. Sequentially, bulky Mullen dendrons were attached to the chromophore through a Diels−Alder reaction between compound **4** and 2,3,4,5-tetraphenylcyclopenta-2,4-dienone to

generate the fluorescent core (**5**). Finally, following our previous report, itpbn was obtained from intermediate **5** as a white solid in reasonable yields. All the synthesized compounds were fully characterized by NMR, mass spectrometry (MS), and elemental analysis.

The photophysical properties of all the molecules were investigated in dilute solutions (Figure 1). To nearly match the
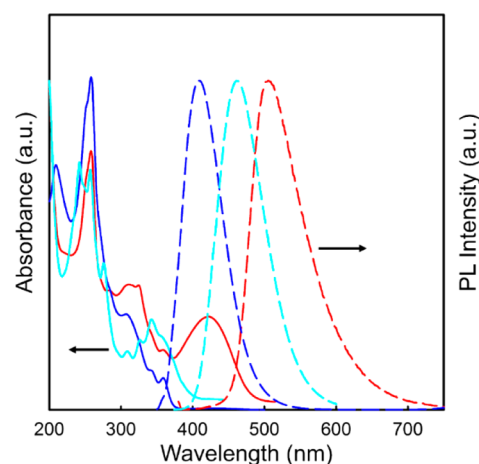
Figure 1. UV−vis absorption (plain lines) and PL spectra (dotted lines): ibpbn (red), itpbn (blue), and ihpypn (cyan) in dilute acetonitrile solutions.

highly polar environment in the LEC active layer, absorption and emission properties were measured in polar acetonitrile solutions. Due to their structural similarity, both the molecules (itpbn and ihpypn) presented similar absorption characteristics. As expected, our emitter turned host molecules itpbn and ihpypn exhibited good photoluminescence quantum yields (Table 1) in dilute acetonitrile solutions.[38] And the absorption

Table 1. Key Photophysical Properties of the Compounds

compd	$\lambda_{PL,max}$[a]	Φ_F[b]	HOMO (eV)[c]	E_g[d]	LUMO (eV)[e]
ibpbn	506	0.002	−5.34	2.59	−2.75
itpbn	409	0.95	−5.32	3.33	−2.0
ihpypn	461	0.63	−5.33	3.09	−2.24

[a]Maximum luminescence in dilute acetonitrile solutions. [b]PLQY measured in acetonitrile (10^{-5} M). [c]Calculated from cyclic voltammetric measurements in DMSO. [d]Optical energy gap calculated from onset of absorbance spectra. [e]Calculated by adding optical energy gap to the HOMO energy level calculated from cyclic voltammetry.

and emission spectra of the these molecules show only negligible change from comparatively less polar tetrahydrofuran to polar acetonitrile, which implies that these molecules have a very small dipolar change in the ground and excited states in polar solvents.[39] This might be due to the less charge-transfer (CT) character of excited states in the molecules, and the energy level responsible for the radiative transition is the locally excited state (LE). Conversely, ibpbn showed a remarkable shift in its emission peak when the solvent polarity was changed. As reported for D−A molecules by several groups, this shift of emission maximum with the solvent polarity may be due to the stabilization of CT excited states.[21,39] In general, emissions can be blue-shifted or red-shifted according to the relative orientation of LE and CT states, if both the states are emissive. In polar solvents, due to its large dipole moment, the CT
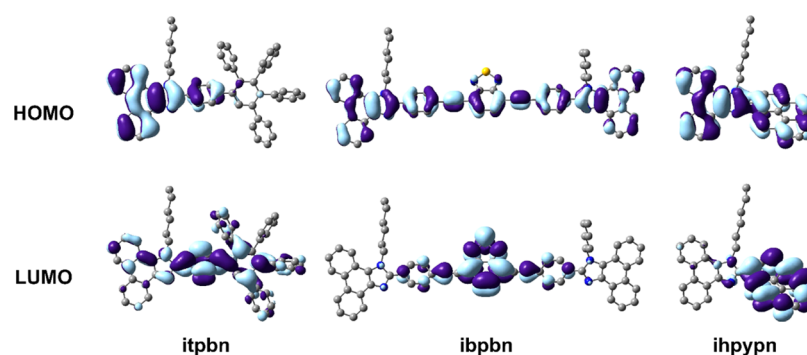
Figure 2. Electron density distribution in the frontier molecular orbitals of the compounds obtained at B3LYP/6-31G (d) level.

excited state can be highly stabilized by solvent molecules and relaxation of the excited state can occur through the CT state radiatively or nonradiatively depending on the level of stabilization of the CT state. This process can occur only when the CT state has lower energy than the LE state.[39] In the case of ibpbn, photoluminescence quantum yield (PLQY) was quenched in polar solvents. With increasing solvent polarity, the fluorescence quantum yield gradually decreased from 0.3 in toluene (489 nm) to 0.002 (506 nm) in acetonitrile. In addition to the typical $\pi-\pi^*$ absorption bands of phenanthroimidazole derivatives, a low-energy typical broad CT peak at 421 nm was observed in the absorption spectrum of ibpbn.[35] When measured in polar acetonitrile, emissions were observed around 506 nm. On the other hand, in moderately polar dichloromethane as solvent, the emission spectra exhibited a dual peak rather than a single maximum indicating an equal contribution from LE and CT excited states (Figure S1); with further decrease in polarity, the emission maximum shifted toward the longer wavelength region (hexane, 591 nm), probably due to more productive relaxation from low-lying CT excited states, which are less stabilized by neutral solvent molecules at this state. From these observations along with previous reports,[21,35,39,40] we concluded that a dominant low-lying CT state exists in this molecule, which is stabilized by solvent dipoles in the highly polar environment, causing nonradiative relaxation from CT excited states. On the other hand, in neutral solvents, the CT state becomes the dominant channel for emission. This observation is problematic considering that the active layer of LECs may act like a high-polarity solvent, and quenching of fluorescence can occur when ibpbn is used as a guest emitter in ionic hosts. However, even in the polar acetonitrile, ibpbn shows less intense emission peak ca. 506 nm, which obviously indicates its radiative LE character in polar environments. Nevertheless, its high performance in LEC devices can be hindered by the deleterious nonradiative relaxation channel existing in this molecule. In the case of host molecules, emission in acetonitrile was centered around 409 and 461 nm, respectively, for ibpbn and itpbn. Consistent with their molecular design, the optical band gaps calculated from the onset of absorption spectra were 2.59, 3.33, and 3.09 eV for ibpbn, itpbn, and ihpypn, respectively. Interestingly, ibpbn exhibited a sharp emission peak at 583 nm (Figure S2) in its thin film, full width at half-maximum (fwhm) around 11 nm when excited at 292 nm. Since the excitation wavelength is exactly the half of the emission peak, the observed signal may be due to a harmonic of the excitation source rather than lasing action of this dye in thin film.[41] Further analysis revealed that this interesting property can be observed only in its thin solid

film, not in solution state. Since the strategies to utilize this property of dyes in LECs are unknown so far and thus, we decided not to investigate it further.

To better understand the electronic properties of synthesized molecules, density functional theory (DFT) calculations were performed with the B3LYP[42,43] functional in conjugation with the 6-31G(d) basis set. Similar to our previous report, herein too, the ionic end groups were omitted to avoid misleading results.[23] For comparative purpose, electronic structures of ihpypn were recalculated in this report. The calculated vibrational spectra have no imaginary frequencies, which indicates that the three optimized structures are located at a minimum point on the potential energy surface. Using the optimized ground-state geometries obtained at the B3LYP/6-31G(d) level, the electronic absorption spectra and emission data were obtained with time-dependent DFT (TDDFT) formalism at the CAM-B3LYP5/6-31G(d) level of theory. The experimental acetonitrile solution was mimicked by using the polarizable continuum model[43,44] to obtain the UV−vis absorption spectra (Figure S3). The DFT-optimized structures of our target molecules are presented in Figure S4. As expected from photophysical studies, both the blue emitters do not show well-segregated highest occupied molecular orbital (HOMO) and lowest unoccupied molecular orbital (LUMO) distributions (Figure 2). The deep-blue host, itpbn, adopted a highly twisted configuration. Along with the ionic side chain, this twisted structure of itpbn may reduce intermolecular interactions in the solid state.[23] Even though intermolecular interactions are detrimental in solution-processable electroluminescent devices due to aggregation-induced quenching of fluorescence in the solid state, host materials having controlled intermolecular interactions are highly desirable to regulate charge transport in the active layer of LEC devices.[45] Being our previous best emitter, ihpypn has already proven to be a potential candidate to the LEC domain. Compared to itpbn, ihpypn may show more intermolecular interactions in the solid state due to the fused rings of pyrene and phenanthroimidazole moieties.[32] The calculated dihedral angles are depicted in Figure S4. In the case of ibpbn, DFT-calculated electronic distributions indicate a separated HOMO and LUMO energy distribution with reasonable overlaps. According to DFT, the HOMO is distributed mainly over the phenanthroimidazole donor, while the LUMO is segregated over the electron-deficient benzothiadiazole acceptor and acetylene bridges. The acceptor and phenyl π bridge are positioned nearly planar in this molecule due to the ethylene bridge, which decreases steric hindrance between peripheral hydrogen atoms. Additionally, the dihedral angle calculated between donor phenanthroimida-

zole and π-bridge was only 31°. This finding underlines the fact that a low-energy CT excited state dominates in the molecule. In polar solvents like acetonitrile the CT state is stabilized and allows a nonradiative relaxation path into the ground state, while maintaining a less dominant productive LE state intact.[34] The calculated HOMO energies (ca. −5.40 eV) of the three compounds are in line with the experimentally determined HOMO energy levels from cyclic voltammetric studies. The DFT-calculated LUMO energy levels (Table S1) of the three compounds have shown little deviation from the experimental results, maybe due to the unreliability of the Kohn−Sham LUMO eigenvalues.[46,47] Absorption spectra of all the compounds were predicted by TDDFT (see Figure S3 and Table S2). The singlet energy gaps were calculated to be 2.12, 3.58, and 3.17 eV for ibpbn, itpbn, and ihpypn, respectively. The corresponding triplet energy levels are estimated to be 1.44, 2.79, and 2.06 eV, respectively, for ibpbn, itpbn, and ihpypn. As expected from the molecular orientation and distribution of frontier molecular orbitals, increased energy differences were found between the lowest singlet (S_1) and triplet excited state (T_1) for all the target molecules. Therefore, thermally activated delayed fluorescence (TADF) is less likely to happen in these molecules.[24]

Furthermore, the findings from DFT calculations of all the molecules were confirmed experimentally through cyclic voltammetry studies using ferrocene as internal standard. All the measurements were carried out in high-purity DMSO solvent with tetrabutylammonium hexafluorophosphate as electrolyte. For all the molecules, oxidation onset was found similar around 1.0, 0.98, and 0.99 V, respectively, for ibpbn, itpbn, and ihpypn (Figure S5). Thus, this confirmed the finding from DFT, that is, HOMO energy levels are distributed mainly on the common phenanthroimidazole moieties. The corresponding HOMO energy levels were calculated using the equation $E_{HOMO} = -4.34 - E_{onset(Ox)}$[32] and found to be −5.34, −5.32, and −5.33 eV for ibpbn, itpbn, and ihpypn, respectively. Additionally, the LUMO energy levels were estimated by adding the optical energy gap (E_g) to the calculated HOMO values. The corresponding LUMO levels are −2.75, −2.0, and −2.24 eV, respectively, for ibpbn, itpbn, and ihpypn.

The application of these molecules in LEC devices was investigated in the device configuration of indium−tin oxide (ITO)/PEDOT:PSS/active layer/Al. On the basis of components in the active layer, three different types of devices were fabricated: (1) ibpbn doped in ihpypn, (2) ibpbn doped in itpbn, and (3) ibpbn as a sole component. Since the molecules used in our devices do not meet the qualities to present thermally activated delayed fluorescence, the majority of electroluminescence may occur through energy transfer from host to dopant via Forster energy transfer due to sufficient spectral overlap between host emission and guest absorption.[48] However, both Forster and Dexter energy transfers are possible to happen. In the absence of RISC, the latter mechanism may act like one among the exciton loss channels in our host−dopant LEC devices. Devices 1−4 have the ihpypn (host)−dopant (ibpbn) system in varying ratios of guest molecules (ibpbn), whereas devices 5 and 6 have itpbn as host and ibpbn as doped emitter. Additionally, an LEC device with ibpbn as a single component was fabricated to investigate its properties as an active material in LECs (device 7). Ratios of ibpbn in these devices were tuned to get maximum luminescence: the active layer of the devices contain 0.3%, 0.6%, 0.9%, and 1.2% of emitter doped in ihpypn, respectively, for devices 1, 2, 3, and 4.

For devices 5 and 6, respectively, 0.6% and 0.9% of emitters were used. Except the solvent used to process the active layer for device 7, a general procedure was adopted to engineer all the devices from 1 to 7. It involves spin-casting a layer of PEDOT:PSS [poly(3,4-ethylenedioxythiophene)−poly-(styrenesulfonate)] on top of an ITO anode, followed by depositing an active layer of our organic molecules from solution. Sequentially, a 100 nm aluminum layer was vacuum-vaporized on top of the active layer to complete the target LEC device structure.

On bias, the constructed LEC devices 1−4 revealed the majority of emission from the doped guest with a shoulder on its left corresponding to the host emissions. When increasing the dopant concentration from devices 1−4, there is an obvious red shift of the emission spectrum, which is common among typical D−A intramolecular charge-transfer (ICT) organic molecules.[24] Furthermore, the emission intensity from the host was observed to be decreasing with increasing emitter ratio. This is a clear indication of increased energy transfer from host to dopant.[49] Particularly in this case, the effects of environmental polarity on the emission spectrum of ibpbn were expected from photophysical characterizations. The electroluminescence (EL) spectra of these LECs are portrayed in Figure 3, and the corresponding data are compiled in Table 2.
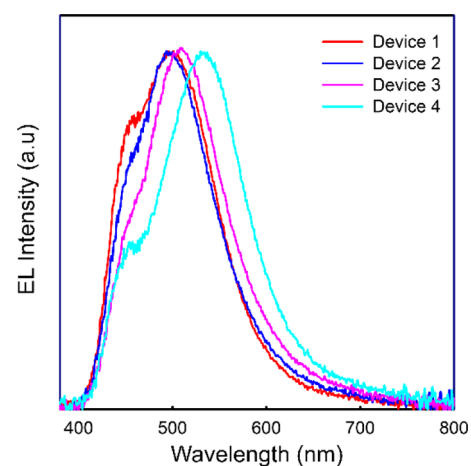
Figure 3. Electroluminescence spectra of LEC devices 1−4.

In comparatively very dilute state (in devices 1 and 2) the EL emission of the ibpbn spectrum marginally changed from its

Table 2. EL Characteristics of the Fabricated LEC Devices 1−7

device	EL$_{max}$[a]	V$_{on}$ (V)[b]	L$_{max}$ (cd m^{-2})[c]	eff$_{max}$ (cd A^{-1})[d]	CIE (x, y)[e]
1	496	6	3795 (0.30)	0.62 (2986)	0.20, 0.33
2	496	7	5016 (0.73)	1.35 (1609)	0.23, 0.37
3	509	7.2	2239 (0.48)	0.81 (434)	0.23, 0.39
4	532	9.2	2166 (0.37)	1.38 (221)	0.29, 0.43
5		10.5	92 (0.04)	0.04 (92)	0.22, 0.23
6		10.5	54 (0.02)	0.02 (54)	0.23, 0.28
7	622	4	30 (0.005)	0.005 (30)	0.54, 0.45

[a]Maximum luminescence. [b]Turn-on voltages at 1 cd m^{-2}. [c]Maximum luminescence (current efficiency in cd A^{-1} at maximum luminescence is given in parentheses). [d]Maximum efficiency (brightness in cd m^{-2} at maximum efficiency is in parentheses). [e]Commission International de l'Eclairage coordinates (CIE) measured at 50 mA.
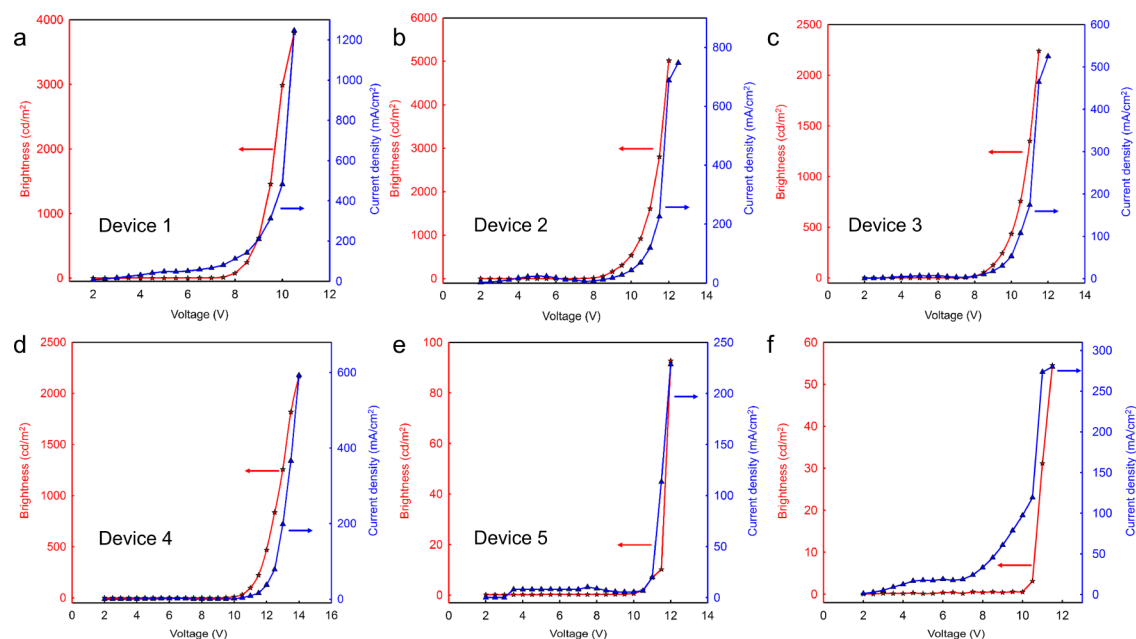
Figure 4. Current density−voltage−luminescence (J−V−L) characteristics, brightness (red line), and current density (blue line) of the LECs devices 1−6.
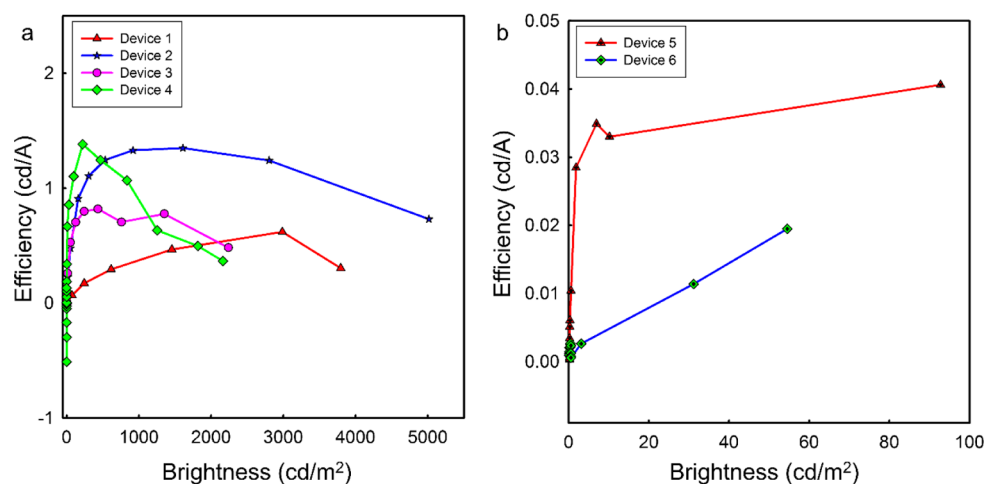
Figure 5. Current efficiency vs brightness of LECs (a) devices 1−4 and (b) devices 5 and 6.

solution emission in acetonitrile, whereas the EL spectrum shows a red shift of 13 and 36 nm in devices 3 and 4, respectively, vide supra. The corresponding CIE (Commission International de l'Eclairage) coordinates were found to be (0.20, 0.33), (0.23, 0.37), (0.23, 0.39), and (0.29, 0.43), respectively, for devices 1, 2, 3, and 4. Depending on the intensity of emission from the host, CIE coordinates of these devices shift from the blue-green to green spectral region. As a result of emission from the host, the color purity exhibited by these devices was poor. Nevertheless, bright electroluminescence was observed from these devices. The maximum brightness exhibited from devices 1, 2, 3, and 4 was 3795, 5016, 2239, and 2166 cd/m^2, respectively (Figure 4). The decreased brightness of devices 3 and 4 may have occurred due to aggregation-induced quenching of fluorescence of emitting species.[24] The turn-on voltage [defined as voltage at which brightness (B) > 1 cd/m^2] was calculated to be 6, 7, 7.2, and 9.2 V for devices 1, 2, 3, and 4, respectively. In addition, maximum current efficiencies were calculated to be 0.62 (B = 2986 cd/

m^2), 1.35 (B = 1609 cd/m^2), 0.81 (B = 434 cd/m^2), and 1.38 cd/A (B = 221 cd/m^2), respectively, for devices 1−4 (Figure 5). Comparatively, high efficiencies at reasonable brightness of device 2 indicate the need for low emitter concentration in the active layer to obtain an efficient and bright host−dopant LEC devices with a D−A emitter. Even then, a generalized conclusion shall not be produced by this single report. However, these maximum brightness and efficiency values exceeded our previous best nondoped LEC device functioned with ihpypn as active material.[23] It is noteworthy that the peak luminescence (device 2) achieved in here is the best among small organic molecule based LECs reported so far[6,13,23,28,31,36,50] and is comparable to the highest luminescent polymer light-emitting electrochemical cells (PLECs)[14,15] and iTMC-LECs.[7,51]

To investigate the possibilities of reverse energy transfer from guest to host having close energy gaps, we fabricated LECs with itpbn as the high band gap host and ibpbn as the emissive component. In contrast to the previous devices,

electroluminescent performances were poor, and in this case too, the emission from the host molecules was sustained in their EL spectra (Figure S6). Dual-wavelength emission pushed the CIE coordinates toward the white region, (0.22, 0.23) and (0.23, 0.28) for devices 5 and 6, respectively. Maximum brightness and maximum efficiencies achieved for the device having 0.6% emitter (device 5) were only around 92 cd/m^2 and 0.4 cd/A, respectively. With further increase in concentration up to 0.9% of emitter (device 6), maximum electroluminescence and maximum efficiency got reduced to 54 cd/m^2 and 0.02 cd/A, respectively. By consolidating the electroluminescent data from devices 1−6, we concluded that undesired emissions from the host can be due to high quantum efficiencies of host molecules compared to guest emitters. A similar, but nonsevere case was observed earlier in quantum dot−polymer (host−dopant) LECs.[52] As reported previously for host materials, the low performance of itpbn devices is attributed to their inability to undergo redox reactions in the active layer of LEC devices.[29] Unlike devices 1−4, LECs fabricated with itpbn show pronounced fluctuations in current density with the increase of voltage. Additionally, $I-V-L$ characteristics of devices 5 and 6 clearly demonstrate that charge transport through the active layer of itpbn is not an easy process (Figure 4). Further scrutinized studies are necessary to identify whether its highly twisted structure has any influence on its low performance in LECs. Finally, an LEC device was fabricated with ibpbn to understand the effect of the host on the performance of those host−dopant LECs. The maximum brightness of this device was only 30 cd/m^2 at a rather low efficiency of 0.005 cd/A (Figure S7). Low luminescence at high current density indicates that quenching of fluorescence may be dominant in this D−A-type emitter, which is intrinsic among D−A semiconductors.[24] Interestingly, the emission color of device 7 (Figure S8) shows similar characteristics to ibpbn in nonpolar hexane, i.e., the majority of emission originated from its CT states, just like its fluorescence from the unpolarized CT state in nonpolar solvents. Thus, aggregation-induced quenching in the active layer is likely to be the competent mechanism of quenching in this red-emitting LEC device (λ_{max} = 622 nm, CIE= 0.54, 0.45).

CONCLUSIONS

Bright electroluminescence from LEC devices can be achieved with potential phenanthroimidazole derivatives. Doping a suitable emitter in an LEC-compatible host is the key in realizing bright electroluminescence from these low-cost solution-processable lighting devices. The performance of these devices is hugely relied on the properties of the host material used rather than the guest emitter; therefore, our host material (ihpypn) can be used to generate strong electroluminescence from a wide range of suitable luminescent materials. Polarization of the CT state can happen when D−A molecules are doped in an ionic host, and thus their CT transfer excited state may act like exciton loss channels in LECs. Fine modulation of CT energy levels in D−A small molecular systems is inevitable in realizing efficient and bright monochromatic light emission from doped D−A LECs. Significant brightness with a less efficient fluorescent emitter indicates the importance of separating the functions of charge transport and recombination in LECs when small fluorescent molecules are used as functional materials. It is noteworthy that all the devices in the ihpypn series (devices 1−4) exhibited much better performance than our previously reported

nondoped ihpypn-only LEC. Notably, being the best performer, device 2 has presented a maximum brightness of 5016 cd/m^2 at an efficiency of 0.73 cd/A. Furthermore, the same device achieved a maximum efficiency of 1.35 cd/A at a brightness of 1609 cd/m^2. In comparison to its host-only device, around a 7-fold increase in the maximum brightness and over a 3-fold increase in the current efficiency at peak brightness were presented by device 2. Irrespective of the color and charge of material used, the maximum brightness achieved by device 2 is the best reported brightness for small organic molecule light-emitting electrochemical cells. Even though the prototype device performance was promising, the design strategy adopted for our emitter may not be satisfactory to meet the requirements for a state-of-the-art D−π-A−π-D due to the flattening of the acceptor and Ph-bridge. Therefore, further efforts should be focused on suppressing undesirable non-radiative relaxational channels by controlling the twisting angles between the aromatic π-segments. In addition, designing a D−π-A−π-D intermolecular charge transferring chromaphoric system with a small energy gap between the lowest singlet and triplet energy levels (ΔE) as well as a large fluorescence rate (k_F) can significantly improve the device performance.

EXPERIMENTAL SECTION

Materials and Methods. All the chemicals and solvents were purchased from commercial suppliers and used without further purifications. Reactions were all carried out under an argon atmosphere using Schlenk apparatus. ^{1}H NMR spectra were recorded on a Varian Unity Inova 500 MHz FT-NMR spectrometer using [D$_6$]DMSO as solvent. Elemental analyses were measured on a Vario LE-III microanalyzer. Mass spectra were obtained from an FAB high-resolution MS/MS system. Absorption spectra were measured using a 8453 UV−vis Agilent spectrophotometer. Thin-film and solution photoluminescence spectra were recorded with an F-7000 FL spectrophotometer. The solution PLQYs were measured in anhydrous acetonitrile (10^{-5} M) with diphenyl anthracene as standard (Φ_F = 0.9 in cyclohexane) for itpbn and ihpypn, whereas solution quantum yield measurements were performed with rhodamine 6G (Φ_F = 0.95 in ethanol) as standard for ibpbn. Thin films for PL measurements were prepared by spin-casting a solution (20 mg/mL in butanol/DMF, 1:3) of ibpbn onto glass substrate, sequentially annealed at 80 °C under vacuum. The onset of absorption spectra was calculated as the intersection of the baseline with the tangent of the longest wavelength peak at the half-maximum of its peak value. The thin-film thickness was measured using an interferometer. Voltammetric measurements were performed in a potentiostat/galvanostat (Iviumstat) voltammetric analyzer using a 10^{-3} M solution of DMSO at a scan rate of 50 mV s^{-1}. The electrolytic cell consisted of glassy carbon as the working electrode, platinum wire as the counter electrode, and Ag/AgCl as the reference electrode. The supporting electrolyte was 0.1 M tetrabutylammonium hexafluorophosphate (TBAPF$_6$) in DMSO, and the redox potentials were measured against the ferrocenium/ferrocene (Fc$^+$/Fc) couple as the internal standard.

The ground-state geometries of the three compounds were estimated by employing DFT with the B3LYP1-3 functional in conjugation with the 6-31G(d) basis set. All the simulations were performed with the Gaussian 09 quantum chemical program. The electronic absorption spectra and emission data were obtained with TDDFT formalism at the CAM-B3LYP5/6-

31G(d) level of theory. The experimental acetonitrile solution was mimicked by using the polarizable continuum model to obtain the UV−vis absorption spectra.

Device Fabrication and Characterization. All the device fabrication and characterizations were carried out in ambient air and moisture conditions. LECs were prepared on commercially available ITO-coated glass substrates. Area for each LEC device is (2 × 5) mm. Initially, ITO patterned glass substrates were ultrasonicated sequentially in detergent, acetone, ethanol, and isopropyl alcohol. After drying at 100 °C, a 60−90 nm PEDOT:PSS layer was spin-coated on top of the ITO anode as a buffer layer and then dried in a vacuum oven at 100 °C for 30 min. For preparing active layers of devices 1−4, a 2 wt % solution of ihpypn in acetonitrile was prepared and the corresponding volume of stock solution (0.12 wt %) of ibpbn in acetonitrile was added. Correspondingly, solutions for devices 5 and 6 were prepared replacing ihpypn with itpbn. For device 7, a 2 wt % solution of ibpbn was prepared in DMF/butanone (3:1) mixture. All the solutions were freshly prepared prior to spin coating of active layers (2000 rpm, 20 s). The resulting active layers were dried at 80 °C for 1 h in high vacuum. On top of the active layers, aluminum cathodes were thermally evaporated using a ULVAC VPC-260 machine at a pressure of 8 × 10⁻³ Pa.

Constant voltage scan was employed for investigating the performance of our devices. The electroluminescence properties of those fabricated LEC devices were measured using a Keithley 2400 source coupled with an OPC 2100 optical spectrum analyzer.

Synthesis and Characterization. *4,4′-(Benzo[c][1,2,5]-thiadiazole-4,7-diylbis(ethyne-2,1-diyl))dibenzaldehyde (1).* 4-Ethynylbenzaldehyde (0.3 g, 2.31 mmol), 4,7-dibromobenzo-[*c*]-1,2,5-thiadiazole (0.339 g, 1.15 mmol), bis-(triphenylphosphine)palladium(II) dichloride (0.03 g, 0.04 mmol), and copper iodide (0.03 g, 0.16 mmol) were added to a Schlenk tube and stirred at 60 °C in a mixture of 20 mL of tetrahydrofuran/triethylamine (1:1) under an argon atmosphere. After a stirring period of 12 h, the precipitated solid was filtered and dissolved in boiling THF and insoluble materials were filtered off. The resultant solution was passed through a silica plug to obtain the product as a yellow solid. Yield: 0.225 g (50%). ^{1}H NMR (400 MHz, [D$_6$]DMSO) δ (ppm): 7.86 (d, J = 8 Hz, 4 H), 7.99 (d, J = 8.4 Hz, 4 H), 8.05 (s, 2 H), 10.04 (s, 2 H). MS (FAB, m/z): [M + H]$^+$ calcd for C$_{24}$H$_{12}$N$_2$O$_2$S, 393.06; found, 393.08. Anal. Calcd for C$_{24}$H$_{12}$N$_2$O$_2$S: C, 73.45; H, 3.08; N, 7.14. Found: C, 71.13; H, 3.10; N, 7.20.

4,7-Bis((4-(1H-phenanthro[9,10-d]imidazol-2-yl)phenyl)-ethynyl)benzo[c][1,2,5]thiadiazole (2). 9,10-Phenanthrenequi-none (0.637 g, 3.06 mmol) and ammonium acetate (1.8 g, 23.35 mmol) were added to a round-bottomed flask containing compound 1 (0.3 g, 0.765 mmol). The mixture was refluxed in 40 mL of glacial acetic acid under an argon cover for 24 h. The obtained red solid was filtered and washed with methanol, dissolved in boiling THF, and insoluble materials were filtered off. Finally, the crude product was obtained as a red solid after precipitating in methanol, filtered, and dried in vacuum. Yield: 0.41 g (70%). ^{1}H NMR (400 MHz, [D$_6$]DMSO) δ (ppm): 7.64 (t, J = 7.6 Hz, 4 H), 7.74 (t, J = 7.4 Hz, 4 H), 7.88 (d, J = 8.4 Hz, 4 H), 8.04 (s, 2 H), 8.41 (d, J = 8.4 Hz, 4 H), 8.55 (d, J = 7.6 Hz, 4 H), 8.85 (d, J = 8.4 Hz, 4 H), 13.59 (br s, 2 H). MS (FAB, m/z): [M + H]$^+$ calcd for C$_{52}$H$_{28}$N$_6$S, 769.21; found, 769.21. Anal. Calcd for C$_{52}$H$_{28}$N$_6$S: C, 81.23; H, 3.67; N, 10.93. Found: C, 81.02; H, 3.55; N, 9.88.

4,7-Bis((4-(1-(6-bromohexyl)-1H-phenanthro[9,10-d]-imidazol-2-yl)phenyl)ethynyl)benzo[c][1,2,5]thiadiazole (3). To a solution of compound 2 (0.25 g, 0.33 mmol) in 25 mL of THF under an argon atmosphere was added sodium hydride (60% in mineral oil, 0.45 g, 18.75 mmol) in batches. After the mixture was refluxed for 30 min, 1,6-dibromohexane (1 mL, 6.5 mmol) was added dropwise via syringe. Following a stirring period of 12 h at 60 °C, another portion of sodium hydride (60% in mineral oil, 0.45 g, 18.75 mmol) was added and stirred until the color of the solution turned brown to yellow (approximately 12 h from the second addition of base). The reaction was quenched by slow addition of methanol (vigorous reaction); the resultant mixture was dissolved in dichloromethane, and the organic layer was washed several times with water; after drying over anhydrous sodium sulfate and concentrating under reduced pressure, the residue was purified by column chromatography on basic alumina (ethyl acetate/hexane, 70:30). Yield: 0.16 g (44%). ^{1}H NMR (400 MHz, [D$_6$]DMSO) δ (ppm): 1.26−1.19 (m, 8 H), 1.13−1.13 (m, 4 H), 1.78−1.70 (m, 4 H), 1.98−1.91 (m, 4 H), 4.68 (t, J = 7.2 Hz, 4 H), 7.71−7.62 (m, 9 H), 7.89−7.81 (m, 9 H), 8.24 (d, J = 8.0 Hz, 2 H), 8.69 (d, J = 7.7 Hz, 2 H), 8.79 (d, J = 7.2 Hz, 2 H), 8.84 (d, J = 7.6 Hz, 2 H). MS (FAB, m/z): [M + H]$^+$ calcd for C$_{64}$H$_{50}$Br$_2$N$_6$S, 1095.22; found, 1095.23. Anal. Calcd for C$_{64}$H$_{50}$Br$_2$N$_6$S: C, 70.20; H, 4.60; N, 7.67. Found: C, 69.78; H, 4.63; N, 7.60.

1,1′-((2,2′-((Benzo[c][1,2,5]thiadiazole-4,7-diylbis(ethyne-2,1-diyl))bis(4,1-phenylene))bis(1H-phenanthro[9,10-d]-imidazole-2,1-diyl))bis(hexane-6,1-diyl))bis(3-methyl-1H-imi-dazol-3-ium) Hexafluorophosphate(V) (ibpbn). Compound 3 (0.15 g, 0.13 mmol) was dissolved in 5 mL of 1-methylimidazole under an argon atmosphere and heated to reflux. After 3 h, the reaction mixture was poured into excess ethyl acetate, the precipitate was filtered, dissolved in a minimum amount of methanol, and ammonium hexafluor-ophosphate (0.04 g, 0.26 mmol) was added to the stirring solution. After 30 min, the solid was filtered; purification was done by column chromatography on alumina (2−10% methanol in dichloromethane). Yield: 0.1 g (55%). ^{1}H NMR (400 MHz, [D$_6$]DMSO) δ (ppm): 1.12−1.0 (m, 8 H), 1.63−1.55 (m, 4 H), 1.88−1.74 (m, 4 H), 3.76 (s, 6 H), 3.99 (t, J = 7.2 Hz, 4 H), 4.74 (t, J = 6.4 Hz, 4 H), 7.79−7.59 (m, 12 H), 7.94−7.88 (m, 8 H), 8.08 (s, 2 H), 8.42 (d, J = 8.4 Hz, 2 H), 8.59 (d, J = 7.6 Hz, 2 H), 8.86 (d, J = 8.4 Hz, 2 H), 8.98 (d, J = 8.8 Hz, 4 H). MS (FAB, m/z): [M − PF$_6$]$^+$ calcd for C$_{72}$H$_{62}$N$_{10}$S^{2+}, 549.24; found, 549.24. Anal. Calcd for C$_{72}$H$_{62}$F$_{12}$N$_{10}$P$_2$S: C, 62.24; H, 4.50; N, 10.08. Found: C, 62.20; H, 4.33; N, 9.90.

2-(4-Ethynylphenyl)-1H-phenanthro[9,10-d]imidazole (4). 9,10-Phenanthrenequinone (1 g, 4.8 mmol) and ammonium acetate (4.5 g, 58.38 mmol) were added to a round-bottomed flask containing 4-ethynylbenzaldehyde (0.62 g, 4.8 mmol). The mixture was refluxed for 12 h in 25 mL of glacial acetic acid under an argon atmosphere. The precipitated solid was filtered, washed with hexane, and purified through column chromatography on silica (ethyl acetate/hexane, 25:75). Yield: 1.07 g (70%). ^{1}H NMR (400 MHz, [D$_6$]DMSO) δ (ppm): 4.33 (s, 1 H), 7.64−7.59 (m, 2 H), 7.73−7.67 (m, 4 H), 8.32−8.28 (m, 2 H), 8.54 (d, J = 8.0 Hz, 2 H), 8.82 (d, J = 8.0 Hz, 2 H), 13.52 (br s, 1 H). MS (FAB, m/z): [M + H]$^+$ calcd for C$_{23}$H$_{14}$N$_2$, 319.12; found, 319.12. Anal. Calcd for C$_{23}$H$_{14}$N$_2$: C, 86.77; H, 4.43; N, 8.80. Found: C, 86.22; H, 4.33; N, 8.85.

2-(3′,4′,5′-Triphenyl-[1,1′:2′,1″-terphenyl]-4-yl)-1H-phenanthro[9,10-d]imidazole (5). Compound **4** (0.7 g, 2.2 mmol) and tetraphenylcyclopentadienone (0.84 g, 2.2 mmol) were added to a round-bottomed flask, which were then refluxed for 24 h in 35 mL of *o*-xylene under an argon cover. After completion of the reaction, hexane was added, and the precipitated solid was filtered and purified through column chromatography on silica (ethyl acetate/hexane, 50:50). Yield: 0.71 g (48%). ^{1}H NMR (400 MHz, [D$_6$]DMSO) δ (ppm): 6.99−6.78 (m, 15 H), 7.19−7.11 (m, 5 H), 7.34 (d, J = 8.4 Hz, 2 H), 7.52 (s, 1H), 7.59 (t, J = 7.2 Hz, 2 H), 7.69 (t, J = 6.8 Hz, 2 H), 8.05 (d, J = 8.8 Hz, 2 H), 8.5 (d, J = 6.8 Hz, 2 H), 8.82 (d, J = 7.2 Hz, 2 H), 13.34 (br s, 1H). MS (FAB, m/z): [M + H]$^+$ calcd for C$_{51}$H$_{34}$N$_2$, 675.27; found, 675.30. Anal. Calcd for C$_{51}$H$_{34}$N$_2$: C, 90.77; H, 5.08; N, 4.15. Found: C, 90.78; H, 5.04; N, 4.25.

2-(3′,4′,5′-Triphenyl-[1,1′:2′,1″-terphenyl]-4-yl)-1H-phenanthro[9,10-d]imidazole (6). A mixture of compound **5** (0.7 g, 1.03 mmol) and potassium *tert*-butoxide (0.28 g, 2.5 mmol) in 25 mL of THF was stirred under an argon atmosphere at 50 °C. After 30 min, 1,6-dibromohexane (1.3 mL, 8.24 mmol) was added to the reaction mixture and stirring continued for another 12 h. The resultant mixture was extracted several times with dichloromethane, and the organic phase was washed with water and dried over anhydrous sodium sulfate. Further purification was done by column chromatography on silica (ethyl acetate/hexane, 30:70). Yield: 0.60 g (70%). ^{1}H NMR (400 MHz, [D$_6$]DMSO) δ (ppm): 1.06−0.99 (m, 2 H), 1.18−1.11 (m, 2 H), 1.63−1.56 (m, 2 H), 1.82−1.67 (m, 2 H), 3.35 (t, J = 6.8 Hz, 2 H), 4.57 (t, J = 6.8 Hz, 2 H), 6.99−6.79 (m, 15 H), 7.19−7.09 (m, 5 H), 7.39−7.37(m, 2 H), 7.76−7.52 (m, 7 H), 8.35 (d, J = 8.4 Hz, 1 H), 8.51 (dd, J = 8, 1.6 Hz, 1 H), 8.81 (d, J = 8 Hz, 1 H), 8.9 (dd, J = 8.4, 0.8 Hz, 1 H). MS (FAB, m/z): [M + H]$^+$ calcd for C$_{57}$H$_{45}$BrN$_2$, 837.28; found, 837.31. Anal. Calcd for C$_{57}$H$_{45}$BrN$_2$: C, 81.71; H, 5.41; N, 3.34. Found: C, 81.50; H, 5.34; N, 3.35.

3-Methyl-1-(6-(2-(3′,4′,5′-triphenyl-[1,1′:2′,1″-terphenyl]-4-yl)-1H-phenanthro[9,10-d]imidazol-1-yl)hexyl)-1H-imidazol-3-ium Hexafluorophosphate(V) (7) (itpbn). Compound **6** (0.5 g, 0.60 mmol) was added to a round-bottomed flask. The mixture was heated at 100 °C in 5 mL of 1-methylimidzole for 3 h. After being brought back to room temperature, ammonium hexafluorophosphate (0.1956 g, 1.2 mmol) in distilled water (10 mL) was added with stirring, the mixture was diluted with excess water, stirred for another 30 min, filtered, and purified through column chromatography on basic alumina (2% methanol in dichloromethane). Yield: 0.35 g (60%). ^{1}H NMR (400 MHz, [D$_6$]DMSO) δ (ppm): 1.03−0.95 (m, 4 H) 1.60−1.51 (m, 2 H), 1.76−1.66 (m, 2 H), 3.74 (s, 2 H), 3.97 (t, J = 7.2 Hz, 2 H), 4.57 (t, J = 6.8 Hz, 2 H), 6.97−6.82 (m, 15 H), 7.19−7.13(m, 5 H), 7.37 (d, J = 8.4 Hz, 2 H), 7.51 (s, 1 H), 7.75−7.54 (m, 9 H), 8.35 (d, J = 8 Hz, 1 H), 8.52 (dd, J = 8, 1.2 Hz, 1 H), 8.81 (d, J = 8 Hz, 1 H), 8.94 (dd, J = 7.2, 0.8 Hz, 2 H). MS (FAB, m/z): [M − PF$_6$]$^+$ calcd for C$_{61}$H$_{51}$N$_4^+$, 839.41; found, 839.41. Anal. Calcd for C$_{61}$H$_{51}$F$_6$N$_4$P: C, 74.38; H, 5.22; N, 5.69. Found: C, 75.02; H, 5.20; N, 5.61.

ASSOCIATED CONTENT

Ⓢ Supporting Information

The Supporting Information is available free of charge on the ACS Publications website at DOI: 10.1021/acs.jpcc.6b03710.

PL spectrum in solution, PL spectrum in thin film, DFT-calculated UV−vis absorption spectrum, DFT-optimized structures of target compounds, cyclic voltammograms, EL spectra of devices 5 and 6, L−I−V characteristics of device 7, EL spectrum of device 7, and Tables S1 and S2 (PDF)

AUTHOR INFORMATION

Corresponding Author

*E-mail: choe@pusan.ac.kr. Phone: +8251 510 2396. Fax: +8251 512 8634.

Notes

The authors declare no competing financial interest.

REFERENCES

(1) Hirata, S.; Sakai, Y.; Masui, K.; Tanaka, H.; Lee, S. Y.; Nomura, H.; Nakamura, N.; Yasumatsu, M.; Nakanotani, H.; Zhang, Q.; Shizu, K.; Miyazaki, H.; Adachi, C. Highly Efficient Blue Electroluminescence Based on Thermally Activated Delayed Fluorescence. *Nat. Mater.* **2015**, *14*, 330−336.

(2) Kaji, H.; Suzuki, H.; Fukushima, T.; Shizu, K.; Suzuki, K.; Kubo, S.; Komino, T.; Oiwa, H.; Suzuki, F.; Wakamiya, A.; et al. Purely Organic Electroluminescent Material Realizing 100% Conversion from Electricity to Light. *Nat. Commun.* **2015**, *6*, 8476.

(3) Xue, J. Y.; Izumi, T.; Yoshii, A.; Ikemoto, K.; Koretsune, T.; Akashi, R.; Arita, R.; Taka, H.; Kita, H.; Sato, S.; et al. Aromatic Hydrocarbon Macrocycles for Highly Efficient Organic Light-Emitting Devices with Single-Layer Architectures. *Chem. Sci.* **2016**, *7*, 896−904.

(4) Su, H.-C.; Cheng, C.-Y. Recent Advances in Solid-State White Light-Emitting Electrochemical Cells. *Isr. J. Chem.* **2014**, *54*, 855−866.

(5) Zhang, Z.; Guo, K.; Li, Y.; Li, X.; Guan, G.; Li, H.; Luo, Y.; Zhao, F.; Zhang, Q.; Wei, B.; Pei, Q.; Peng, H. A Colour-Tunable, Weavable Fibre-Shaped Polymer Light-Emitting Electrochemical Cell. *Nat. Photonics* **2015**, *9*, 233−238.

(6) Tang, S.; Tan, W.-Y.; Zhu, X.-H.; Edman, L. Small-Molecule Light-Emitting Electrochemical Cells: Evidence for in Situ Electrochemical Doping and Functional Operation. *Chem. Commun.* **2013**, *49*, 4926−4928.

(7) Meier, S. B.; Tordera, D.; Pertegás, A.; Roldán-Carmona, C.; Ortí, E.; Bolink, H. J. Light-Emitting Electrochemical Cells: Recent Progress and Future Prospects. *Mater. Today* **2014**, *17*, 217−223.

(8) Sunesh, C. D.; Subeesh, M. S.; Shanmugasundaram, K.; Chitumalla, R. K.; Jang, J.; Choe, Y. Synthesis of Heteroleptic Iridium Complexes with Sterically Hindered Methyl Groups on Pyrazole Ligands for Efficient Yellow and Green Light-Emitting Electrochemical Cells. *Dyes Pigm.* **2016**, *128*, 190−200.

(9) Sunesh, C. D.; Shanmugasundaram, K.; Subeesh, M. S.; Chitumalla, R. K.; Jang, J.; Choe, Y. Blue and Blue-Green Light-Emitting Cationic Iridium Complexes: Synthesis, Characterization, and Optoelectronic Properties. *ACS Appl. Mater. Interfaces* **2015**, *7*, 7741−7751.

(10) Su, H.-C.; Hsu, J.-H. Improving the Carrier Balance of Light-Emitting Electrochemical Cells Based on Ionic Transition Metal Complexes. *Dalt. Trans.* **2015**, *44*, 8330−8345.

(11) Cheng, C.-Y.; Wang, C.-W.; Cheng, J.-R.; Chen, H.-F.; Yeh, Y.-S.; Su, H.-C.; Chang, C.-H.; Wong, K.-T. Enhancing Device Efficiencies of Solid-State White Light-Emitting Electrochemical Cells by Employing Waveguide Coupling. *J. Mater. Chem. C* **2015**, *3*, 5665−5673.

(12) Hernandez-Sosa, G.; Tekoglu, S.; Stolz, S.; Eckstein, R.; Teusch, C.; Trapp, J.; Lemmer, U.; Hamburger, M.; Mechau, N. The Compromises of Printing Organic Electronics: A Case Study of Gravure-Printed Light-Emitting Electrochemical Cells. *Adv. Mater.* **2014**, *26*, 3235−3240.

(13) van Reenen, S.; Janssen, R. A. J.; Kemerink, M. Fundamental Tradeoff between Emission Intensity and Efficiency in Light-Emitting Electrochemical Cells. *Adv. Funct. Mater.* **2015**, *25*, 3066−3073.

(14) Xiong, Y.; Li, L.; Liang, J.; Gao, H.; Chou, S.; Pei, Q. Efficient White Polymer Light-Emitting Electrochemical Cells. *Mater. Horiz.* **2015**, *2*, 338−343.

(15) Yu, Z.; Wang, M.; Lei, G.; Liu, J.; Li, L.; Pei, Q. Stabilizing the Dynamic P−i−n Junction in Polymer Light-Emitting Electrochemical Cells. *J. Phys. Chem. Lett.* **2011**, *2*, 367−372.

(16) Sunesh, C. D.; Mathai, G.; Choe, Y. Constructive Effects of Long Alkyl Chains on the Electroluminescent Properties of Cationic Iridium Complex-Based Light-Emitting Electrochemical Cells. *ACS Appl. Mater. Interfaces* **2014**, *6*, 17416−17425.

(17) Chen, H.-F.; Liao, C.-T.; Su, H.-C.; Yeh, Y.-S.; Wong, K.-T. Highly Efficient Exciplex Emission in Solid-State Light-Emitting Electrochemical Cells Based on Mixed Ionic Hole-Transport Triaryl-amine and Ionic Electron-Transport 1{,}3{,}5-Triazine Derivatives. *J. Mater. Chem. C* **2013**, *1*, 4647−4654.

(18) Chen, H.-F.; Liao, C.-T.; Kuo, M.-C.; Yeh, Y.-S.; Su, H.-C.; Wong, K.-T. {UV} Light-Emitting Electrochemical Cells Based on an Ionic 2,2′-Bifluorene Derivative. *Org. Electron.* **2012**, *13*, 1765−1773.

(19) Chen, H.-F.; Liao, C.-T.; Chen, T.-C.; Su, H.-C.; Wong, K.-T.; Guo, T.-F. An Ionic Terfluorene Derivative for Saturated Deep-Blue Solid State Light-Emitting Electrochemical Cells. *J. Mater. Chem.* **2011**, *21*, 4175−4181.

(20) Liu, H.; Bai, Q.; Yao, L.; Zhang, H.; Xu, H.; Zhang, S.; Li, W.; Gao, Y.; Li, J.; Lu, P.; et al. Highly Efficient near Ultraviolet Organic Light-Emitting Diode Based on a Meta-Linked Donor-Acceptor Molecule. *Chem. Sci.* **2015**, *6*, 3797−3804.

(21) Yao, L.; Zhang, S.; Wang, R.; Li, W.; Shen, F.; Yang, B.; Ma, Y. Highly Efficient Near-Infrared Organic Light-Emitting Diode Based on a Butterfly-Shaped Donor−Acceptor Chromophore with Strong Solid-State Fluorescence and a Large Proportion of Radiative Excitons. *Angew. Chem., Int. Ed.* **2014**, *53*, 2119−2123.

(22) Shanmugasundaram, K.; Subeesh, M. S.; Sunesh, C. D.; Choe, Y. Non-Doped Deep Blue Light-Emitting Electrochemical Cells from Charged Organic Small Molecules. *RSC Adv.* **2016**, *6*, 28912−28918.

(23) Subeesh, M. S.; Shanmugasundaram, K.; Sunesh, C. D.; Nguyen, T. P.; Choe, Y. Phenanthroimidazole Derivative as an Easily Accessible Emitter for Non-Doped Light-Emitting Electrochemical Cells. *J. Phys. Chem. C* **2015**, *119*, 23676−23684.

(24) Zhang, Q.; Kuwabara, H.; Potscavage, W. J.; Huang, S.; Hatae, Y.; Shibata, T.; Adachi, C. Anthraquinone-Based Intramolecular Charge-Transfer Compounds: Computational Molecular Design, Thermally Activated Delayed Fluorescence, and Highly Efficient Red Electroluminescence. *J. Am. Chem. Soc.* **2014**, *136*, 18070−18081.

(25) Mindemark, J.; Edman, L. Illuminating the Electrolyte in Light-Emitting Electrochemical Cells. *J. Mater. Chem. C* **2016**, *4*, 420−432.

(26) Li, J.; Nomura, H.; Miyazaki, H.; Adachi, C. Highly Efficient Exciplex Organic Light-Emitting Diodes Incorporating a Heptazine Derivative as an Electron Acceptor. *Chem. Commun.* **2014**, *50*, 6174−6176.

(27) Chen, Z.; Liu, X.-K.; Zheng, C.-J.; Ye, J.; Li, X.-Y.; Li, F.; Ou, X.-M.; Zhang, X.-H. A High-Efficiency Hybrid White Organic Light-Emitting Diode Enabled by a New Blue Fluorophor. *J. Mater. Chem. C* **2015**, *3*, 4283−4289.

(28) Pertegás, A.; Tordera, D.; Serrano-Pérez, J. J.; Ortí, E.; Bolink, H. J. Light-Emitting Electrochemical Cells Using Cyanine Dyes as the Active Components. *J. Am. Chem. Soc.* **2013**, *135*, 18008−18011.

(29) Tang, S.; Buchholz, H. A.; Edman, L. On the Selection of a Host Compound for Efficient Host-Guest Light-Emitting Electrochemical Cells. *J. Mater. Chem. C* **2015**, *3*, 8114−8120.

(30) Pertegas, A.; Shavaleev, N. M.; Tordera, D.; Orti, E.; Nazeeruddin, M. K.; Bolink, H. J. Host-Guest Blue Light-Emitting Electrochemical Cells. *J. Mater. Chem. C* **2014**, *2*, 1605−1611.

(31) Shanmugasundaram, K.; Subeesh, M. S.; Sunesh, C. D.; Chitumalla, R. K.; Jang, J.; Choe, Y. Synthesis and Photophysical Characterization of an Ionic Fluorene Derivative for Blue Light-Emitting Electrochemical Cells. *Org. Electron.* **2015**, *24*, 297−302.

(32) Subeesh, M. S.; Shanmugasundaram, K.; Sunesh, C. D.; Won, Y. S.; Choe, Y. Utilization of a Phenanthroimidazole Based Fluorophore in Light-Emitting Electrochemical Cells. *J. Mater. Chem. C* **2015**, *3*, 4683−4687.

(33) Yuan, Y.; Chen, J.-X.; Lu, F.; Tong, Q.-X.; Yang, Q.-D.; Mo, H.-W.; Ng, T.-W.; Wong, F.-L.; Guo, Z.-Q.; Ye, J.; et al. Bipolar Phenanthroimidazole Derivatives Containing Bulky Polyaromatic Hydrocarbons for Nondoped Blue Electroluminescence Devices with High Efficiency and Low Efficiency Roll-Off. *Chem. Mater.* **2013**, *25*, 4957−4965.

(34) Yao, L.; Pan, Y.; Tang, X.; Bai, Q.; Shen, F.; Li, F.; Lu, P.; Yang, B.; Ma, Y. Tailoring Excited-State Properties and Electroluminescence Performance of Donor−Acceptor Molecules through Tuning the Energy Level of the Charge-Transfer State. *J. Phys. Chem. C* **2015**, *119*, 17800−17808.

(35) Tang, X.; Bai, Q.; Peng, Q.; Gao, Y.; Li, J.; Liu, Y.; Yao, L.; Lu, P.; Yang, B.; Ma, Y. Efficient Deep Blue Electroluminescence with an External Quantum Efficiency of 6.8% and CIEy < 0.08 Based on a Phenanthroimidazole−Sulfone Hybrid Donor−Acceptor Molecule. *Chem. Mater.* **2015**, *27*, 7050−7057.

(36) Hill, Z. B.; Rodovsky, D. B.; Leger, J. M.; Bartholomew, G. P. Synthesis and Utilization of Perylene-Based N-Type Small Molecules in Light-Emitting Electrochemical Cells. *Chem. Commun.* **2008**, 6594−6596.

(37) Kumar, D.; Thomas, K. R. J.; Lin, C.-C.; Jou, J.-H. Pyreneimidazole-Based Deep-Blue-Emitting Materials: Optical, Electrochemical, and Electroluminescent Characteristics. *Chem.—Asian J.* **2013**, *8*, 2111−2124.

(38) Eaton, E. F. Reference Materials for Fluorescence Measurement. *Pure Appl. Chem.* **1988**, *60*, 1107−1114.

(39) Li, W.; Liu, D.; Shen, F.; Ma, D.; Wang, Z.; Feng, T.; Xu, Y.; Yang, B.; Ma, Y. A Twisting Donor-Acceptor Molecule with an Intercrossed Excited State for Highly Efficient, Deep-Blue Electroluminescence. *Adv. Funct. Mater.* **2012**, *22*, 2797−2803.

(40) Tanaka, H.; Shizu, K.; Nakanotani, H.; Adachi, C. Dual Intramolecular Charge-Transfer Fluorescence Derived from a Phenothiazine-Triphenyltriazine Derivative. *J. Phys. Chem. C* **2014**, *118*, 15985−15994.

(41) Huang, J.; Liu, Q.; Zou, J.-H.; Zhu, X.-H.; Li, A.-Y.; Li, J.-W.; Wu, S.; Peng, J.; Cao, Y.; Xia, R.; et al. Electroluminescence and Laser Emission of Soluble Pure Red Fluorescent Molecular Glasses Based on Dithienylbenzothiadazole. *Adv. Funct. Mater.* **2009**, *19*, 2978−2986.

(42) Becke, A. D. Density-functional Thermochemistry. III. The Role of Exact Exchange. *J. Chem. Phys.* **1993**, *98*, 5648−5652.

(43) Becke, A. D. Density-functional Thermochemistry. IV. A New Dynamical Correlation Functional and Implications for Exact-exchange Mixing. *J. Chem. Phys.* **1996**, *104*, 1040−1046.

(44) Miertuš, S.; Scrocco, E.; Tomasi, J. Electrostatic Interaction of a Solute with a Continuum. A Direct Utilizaion of AB Initio Molecular Potentials for the Prevision of Solvent Effects. *Chem. Phys.* **1981**, *55*, 117−129.

(45) He, L.; Duan, L.; Qiao, J.; Dong, G.; Wang, L.; Qiu, Y. Highly Efficient Blue-Green and White Light-Emitting Electrochemical Cells Based on a Cationic Iridium Complex with a Bulky Side Group. *Chem. Mater.* **2010**, *22*, 3535−3542.

(46) Ku, J.; Lansac, Y.; Jang, Y. H. Time-Dependent Density Functional Theory Study on Benzothiadiazole-Based Low-Band-Gap Fused-Ring Copolymers for Organic Solar Cell Applications. *J. Phys. Chem. C* **2011**, *115*, 21508−21516.

(47) Zhang, G.; Musgrave, C. B. Comparison of DFT Methods for Molecular Orbital Eigenvalue Calculations. *J. Phys. Chem. A* **2007**, *111*, 1554−1561.

(48) Baldo, M. A.; O'Brien, D. F.; Thompson, M. E.; Forrest, S. R. Excitonic Singlet-Triplet Ratio in a Semiconducting Organic Thin Film. *Phys. Rev. B: Condens. Matter Mater. Phys.* **1999**, *60*, 14422−14428.

(49) Baldo, M. A.; Forrest, S. R. Transient Analysis of Organic Electrophosphorescence: I. Transient Analysis of Triplet Energy Transfer. *Phys. Rev. B: Condens. Matter Mater. Phys.* **2000**, *62*, 10958−10966.

(50) Wong, M. Y.; Hedley, G. J.; Xie, G.; Kölln, L. S.; Samuel, I. D. W.; Pertegás, A.; Bolink, H. J.; Zysman-Colman, E. Light-Emitting Electrochemical Cells and Solution-Processed Organic Light-Emitting Diodes Using Small Molecule Organic Thermally Activated Delayed Fluorescence Emitters. *Chem. Mater.* **2015**, *27*, 6535−6542.

(51) Bunzli, A. M.; Constable, E. C.; Housecroft, C. E.; Prescimone, A.; Zampese, J. A.; Longo, G.; Gil-Escrig, L.; Pertegas, A.; Orti, E.; Bolink, H. J. Exceptionally Long-Lived Light-Emitting Electrochemical Cells: Multiple Intra-Cation π-Stacking Interactions in $[\text{Ir}(\hat{\text{C}}\text{N})2\text{-}(\hat{\text{N}}\text{N})][\text{PF6}]$ Emitters. *Chem. Sci.* **2015**, *6*, 2843−2852.

(52) Norell Bader, A. J.; Ilkevich, A. A.; Kosilkin, I. V.; Leger, J. M. Precise Color Tuning via Hybrid Light-Emitting Electrochemical Cells. *Nano Lett.* **2011**, *11*, 461−465.